CIRP Journal of Manufacturing Science and Technology 1 (2008) 97–102

Contents lists available at ScienceDirect

CIRP Journal of Manufacturing Science and Technology

journal homepage: www.elsevier.com/locate/cirpj

Application of AE and cutting force signals in tool condition monitoring in micro-milling

K. Jemielniak [a,*], P.J. Arrazola [b]

[a] Warsaw University of Technology, Narbutta 86, 02-524 Warsaw, Poland
[b] Mondragon University, Manufacturing Dept, Basque Country, Spain

ARTICLE INFO

Article history:
Available online 8 November 2008

Keywords:
Micro-milling
Tool condition monitoring
Acoustic emission
Cutting forces

ABSTRACT

The paper presents acoustic emission and cutting force signals application in tool condition monitoring in micro-milling of cold-work tool steel. The results obtained revealed strong influence of tool wear on acoustic emission signal, providing acceptable results even while used separately. The signal was easy to register, and showed a very short reaction time to the tool–workpiece contact. As excitation frequency, equal to edge passing frequency, was much higher than in conventional milling, cutting forces, usually the best for this purpose, were strongly disturbed by resonance vibration of the table dynamometer. Despite these disturbances, the signals still show dependence on tool wear, making them useful for tool condition monitoring.

1. Introduction

The demand for miniaturization in many areas, such as the aerospace, automotive, medical, and electronics industries is increasing. The development of micro-milling process for micro-mould manufacturing is driven by these demands due to its capability of machining 3D free-form micro-structures from highly wear resistant materials that have to be heat treated before micro-cutting to achieve a reasonable surface finish [1]. The flexibility and efficiency of micro-end milling processes using carbide tools allow the fabrication of smaller batches than with other processes. Therefore, measurement and monitoring become critical [2]. While tool wear monitoring has been extensively studied on the macro-scale, very limited work has been conducted at the micro-scale.

In micromachining applications, cutting force components and acoustic emission (AE) are most often used in tool condition monitoring (TCM) systems [1,2]. Since force signals are the best indicators of the state of the machining operation, the majority of researchers who have investigated micromachining processes had used cutting force for monitoring or improving the quality of sculptured products. However, because of the small diameter of the end mill, despite relatively low-cutting speeds, very high-spindle speeds (rpm) are used. As the bandwidth of sensors should be a few times higher than the tooth passing speed cutting force sensing system in microcutting operations can be easily exited with a frequency close to the natural frequency of the system which strongly disturbs the signal.

The noise from disturbance sources that generally contaminates the desired signal can be minimized by using AE sensors, as AE tends to propagate at frequencies well above the characteristic frequencies attributed to machining, such as spindle RPM or natural frequencies. AE is more advantageous then force or vibration especially at the ultraprecision scale, due to its relatively superior signal/noise ratio and sensitivity. Hence, AE is particularly well suited because of its ability to detect microscale deformation mechanisms within a relatively 'noisy' machining environment [3].

A review of earlier TCM developments can be found in [4,5]. The possibility of reliable tool wear evaluation based on one signal feature (SF) has been questioned because the feature may offer incomplete or randomly distorted information about the condition of a cutting tool. Attempts at rectifying these shortcomings have focused primarily on pursuing a multi-sensor fusion strategy, which can be achieved by various means, such as statistical methods, auto-regressive modeling, pattern recognition, expert systems, and others [6,7]. Recently, the neural network (NN) approach has been the most intensively studied method for the feature fusion. Usually, a single NN is used in which several SFs are fed into the network as inputs, while the condition of the tool is the network output. However, the use of many SFs in a single NN requires extensive experimental data that are not available if the TCM system is supposed to be trained during the first tool life and to be ready to monitor the tool during the next ones. A different

* Corresponding author. Tel.: +48 22 660 8656; fax: +48 22 849 0285.
E-mail address: k.jemielniak@cim.pw.edu.pl (K. Jemielniak).

1755-5817/$ – see front matter © 2008 CIRP.
doi:10.1016/j.cirpj.2008.09.007

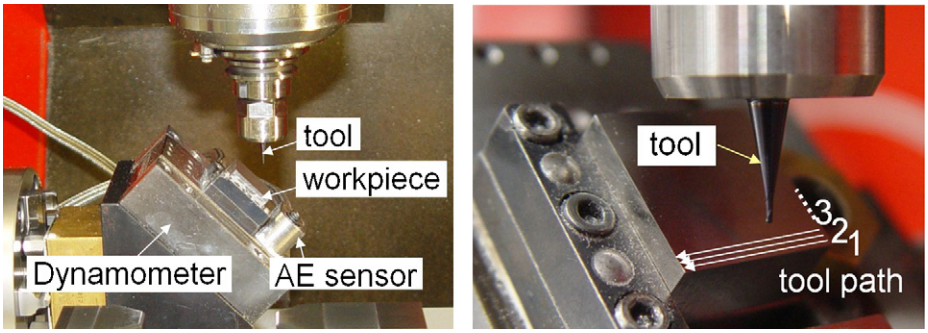

Fig. 1. Experimental setup.

approach is based on hierarchical algorithms [8–10], where a TCM system consists of two modules. The first module estimates the tool wear from all SFs taken from one sensor. The results are then integrated into the final system's response in the second module. In [9,10] the efficiency of TCM strategies based on a single NN with several input signals and on a hierarchical algorithm was analyzed. The latter proved to be much more efficient, which was attributed to inadequate learning data (collected during the first tool life) in relation to the necessary network size. In a system based on hierarchical algorithms, many more SFs can be used, since the SF vs. tool wear function for a single feature is simple, easy to determine, and easy to reverse, while the use of the direct determination of the tool wear vs. (SF_1, ..., SF_N) function requires numerous learning data and a long learning time.

2. Experimental setup and measurements results

The experiments were performed at the Micro-Machining Laboratory at Mondragón University. Fig. 1 shows the experimental setup arranged at a high-precision milling machine, equipped with a 50,000 rpm electrospindle. The workpiece was a cold-work tool steel X155CrVMo12-1, 50 HRC clamped on a three-axis Kistler 9256C1 mini-dynamometer side-by-side with Kistler 8152B221 AE sensor. Cutting forces and AE_{RMS} signals were acquired at a sampling frequency of 50 kHz. Two-flute uncoated micro-grain WC ball end mills with 400 μm radii and 30° helix angle were used for a side-milling operation performed on a 45° tilted workpiece surface 20 × 20 mm in subsequent cuts with cutting parameters: rotational speed n = 36,210 rpm, cutting speed v_c = 68 m/min, feed f_z = 0.016 mm/tooth, depth of cut a_p = 0.05 mm, width of cut a_e = 0.05 mm. Thus one cut lased little more than one second, and the surface was machined in 400 cuts. The total wear in the flank wear VB_{Bmax} = 0.11 mm, was used as the tool life criterion. The test was regularly interrupted to measure the wear in an optic stereo microscope.

Simple tap tests were performed to evaluate the natural frequencies of the dynamometer with the workpiece and AE sensor attached. Spectral analysis of the obtained signals showed (Fig. 2) that apart from the main mode 5080 Hz frequency, much lower frequency modes also existed in the x and y directions.

2.1. Tool life measurements

Four complete tool life tests were performed. Fig. 3 presents an example of the tool wear measurements and flank wear curves from those tests. As Fig. 3 shows, tool lives ranged from 5.7 to 12.2 min. The first and second tool were worn out during the machining of the first surface, while the third and fourth lasted much longer and machined almost two surfaces. Here, the used-up portion of the tool life (ΔT), defined as the ratio of the cutting time as performed so far (t) to the overall tool life span (T), was used as the tool condition measure. So, tool wear measurements were used only to specify the end of tool life—in the case of the first one for system training and in the subsequent ones for testing the system performance. The tool life end can be determined by the operator in any other way that is deemed to be suitable for a particular case.

2.2. Acoustic emission and cutting forces measurements

In Fig. 4 examples of AE_{RMS} and cutting force (F_z here) signal measurements are presented. These were acquired during one cut on the left and during the first 20 ms of the same cut on the right. The AE signal undergoes prominent changes, being much stronger at the beginning and weaker in the middle of a cut, often rising again at the end. These changes can be caused by different AE signal paths or for some other reason out of the control of this experiment. At first glance it seems to be typical burst AE signal registered during cutting. A closer look at these signals reveals however, that the "bursts" appear regularly, at a tooth passing frequency equal to 1207 Hz. The duration of the tool–workpiece contact is so short that any traditional method of AE signal processing, like burst counting, cannot be applied.

It is worth mentioning that a feature of the AE_{RMS} signal registered during the first milliseconds of a cut is the response time to the beginning of the tool engagement with the workpiece. During the first two contacts of the cutting edge with the work, while the uncut chip thickness is so small that the cutting force signals almost do not react, the AE_{RMS} signal rises eminently—up to 55 mV in 0.2 ms. This makes the AE_{RMS} signal robust and a versatile means of detecting the contact between the tool and the part and,

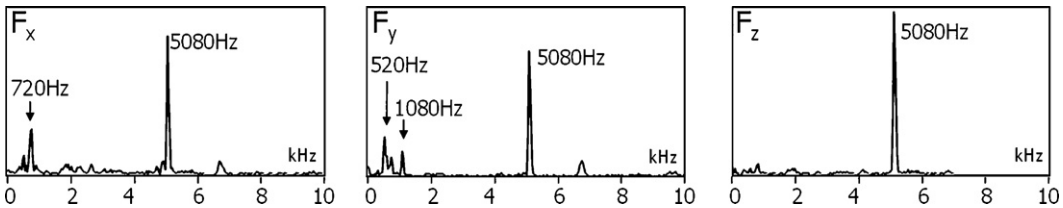

Fig. 2. Dynamometer frequency response to the tap excitation.

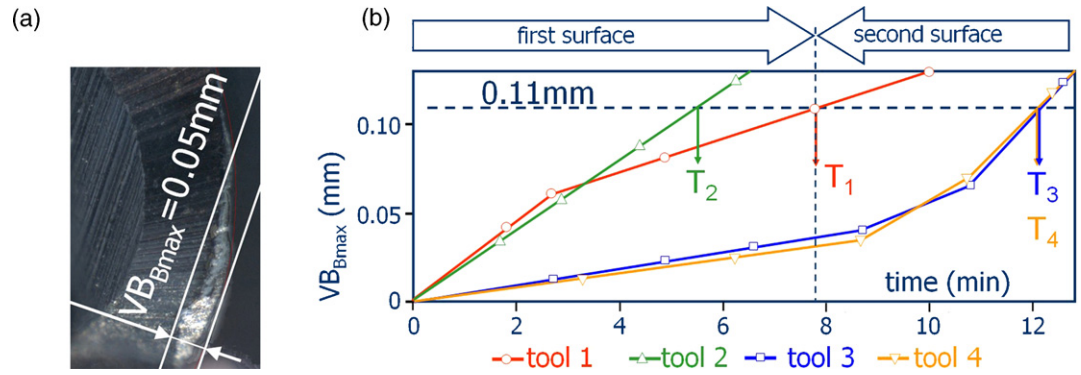

Fig. 3. Tool wear measurement example (a) and development in all tests (b).

thus, the tool integrity (presence, contact with the workpiece) in the process.

The cutting force signals are supposed to change periodically, accordingly to the tool load, so the dominant frequency should be equal to the tooth passing frequency in the case of the absence of tool runout, or spindle speed if the runout is significant. A comparison of these signals with the AE_{RMS} signal reveals however, that the dominant frequency is much higher. In the F_z signal dominates 4828 Hz component—fourth harmonic of the tool passing frequency, closest to the natural frequency of the dynamometer (5080 Hz). It is obvious that the cutting force measurements, as they are, cannot be used for, e.g. modeling of the forces. To find out the real course of the cutting forces, all these disturbances should be removed, e.g. using a Kalman filter [11,12], which – in the case of such distorted measurements as are presented here – would not be very easy anyway. On the other hand, in tool condition monitoring the actual values of the measured feature (cutting force) are not that important. What really counts here is the correlation between the signal features and the tool wear. Therefore, it was decided to try to exploit these distorted signals in tool wear monitoring.

3. Tool wear monitoring

3.1. Signal feature calculation

Numerous signal features (SFs) should be calculated by the TCM system, because it cannot be determined in advance which ones will appear to be useful in a particular application. Therefore, first from all four available signals (AE_{RMS}, F_x, F_y and F_z), nine time domain SFs were calculated for each cut: average value (AE_{av}, F_{xav}, F_{yav}, F_{zav}), RMS value (AE_{rms}, F_{xrms}, ...), standard deviation (AE_{sd}, F_{xsd}, ...), minimum (value below which was 5% of all values, AE_{mi}, F_{xmi}, ...), maximum (value above which was 5% of all values, AE_{mx}, F_{xmx}, ...), range (max–min, AE_{rg}, F_{xrg}, ...), maximum minus average ($AE_{mx\text{-}av}$, $F_{xmx\text{-}av}$, ...), minimum minus average ($AE_{mi\text{-}av}$, $F_{xmi\text{-}av}$, ...), and finally the average of the absolute difference between subsequent signal values (AE_{dY}, F_{xdY}, ...). As the signals are not generally constant, all of the SFs mentioned above were also calculated for the beginning (first 20%) of the cut and for the middle part (40–80%) of the cut, and designated with the letters "bg" or "md" in the indices of the SF's designation, respectively, e.g. AE_{bgmi}, F_{xbgmi}, ... AE_{mdmi}, F_{xmdmi}, ... For cutting force signals, four frequency domain SFs were also calculated for the whole, beginning, and middle parts of the cuts: power in the rpm band (rpm power), e.g. F_{xPrpm}, $F_{xbgPrpm}$, $F_{xmdPrpm}$, power in the edge passing frequency band (edge power), e.g. F_{xPedg}, $F_{xbgPedg}$, $F_{xmdPedg}$, the sum of both, e.g. F_{xsumP}, $F_{xbgsumP}$, $F_{xmdsumP}$, and finally a ratio of the latter two (relative edge power), e.g. F_{xrelP}, $F_{xbgrelP}$, $F_{xmdrelP}$.

There is usually an offset between the SFs, which can be caused by different, uncontrolled values of cutting conditions. Therefore, the first SF value is subtracted from all the SF values for a particular tool life so that all SF courses starts from zero, and only their changes matter.

Altogether 144 signal features were calculated for each cut. Examples of the SFs obtained in this study are presented in Fig. 5. Many of them underwent dramatic changes when the tools (third and fourth) started to machine the second surface (after 400 cuts). Very distorted and not repeatable SF courses is a problem that challenges any tool condition monitoring system.

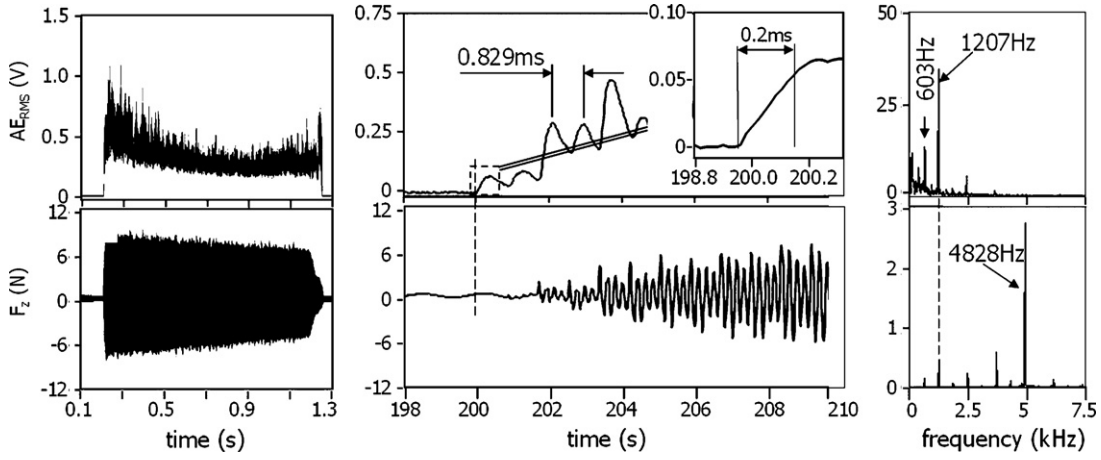

Fig. 4. Examples of acoustic emission and cutting force signals registered during tests.

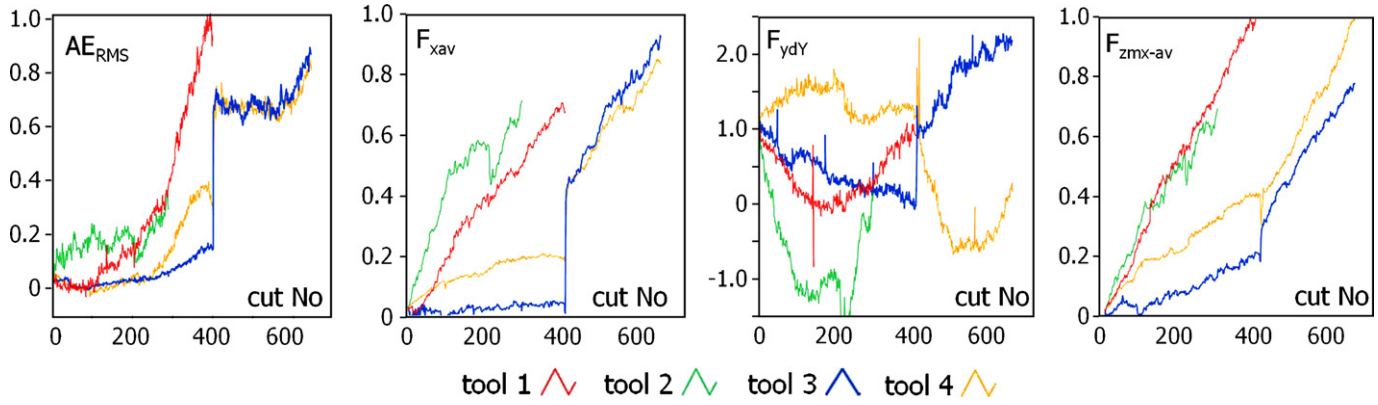

Fig. 5. Examples of SFs obtained in this study, amplitudes are normalized (see text).

3.2. Signal feature selection

Having an ample number of signal features, originating from one or more signals, one should select those that correlate to the tool wear, meaning there is a clear dependence of the feature on the tool wear. It should be stressed that the selection of signal features is always performed using data from the first, training tool life only. In the proposed TCM system, the following method is used. First, the original SF ($F_{xmi\text{-}av}$ in first and third tool life taken as an example; Fig. 6(a)) is normalized in time to 0–100% of tool life to SF_T (see Fig. 6(b)) then low-pass filtered to SF_{Tf} (dotted line in Fig. 6(b)). The SF_{Tf} is an approximation of the SF(ΔT) relationship.

To make the comparison and evaluation of the signal features easier and more transparent, their amplitudes are normalized to a (0:1) range based on the SF_{TF} range in the first tool life. The root mean square error between SF_{Ta} and SF_{Tfa} is a measure of signal feature usability for tool wear monitoring ($RMSE_U$). Features with an $RMSE_U$ higher than 0.2 were rejected from further evaluation. Of course, as the SF vs. ΔT in every tool life differs (which is too bad), feature selection depends on the tool life taken for the system training. Here, when the first tool was the training one, $F_{xmi\text{-}av}$ appeared to be a very good SF ($RMSE_U = 0.050$), while when the third tool life was taken for training, this SF was rejected ($RMSE_U = 0.202$).

Dealing with a large number (144 here) of signal features, it usually appears that, among those that meet the criteria, there are groups of SFs that are similar (correlated) to each other. To eliminate the features that do not contain additional information, the following procedure is applied here. First, the best feature (with the smallest $RMSE_U$) is selected. Then the root mean square errors between this feature and all others, are calculated as measure of similarity ($RMSE_S$), and those with $RMSE_S$ values less than 0.05 are rejected. From among the remaining signal features, again the best one is selected, and the SFs correlated with it are rejected. The procedure is repeated until no signal feature meeting the criterion remains.

In practice, the selection of a signal feature and the training of a system would be performed using data from the first tool life only. However, to verify the proposed TCM system strategy, the whole procedure was repeated four times, each time taking another tool as the first, i.e., training, tool. Thus, we have four separate verification experiments instead of one. Table 1 presents the signal features that were selected automatically in these experiments, and the best and the worst for each tool are presented in Fig. 7. As can be seen there, the same SF selected as good for one tool (tool life) can be rejected for another. It is worth noticing that, despite having nominally the same cutting conditions in all four tests, SF(ΔT) courses are not repeatable, which proves that none of them alone could be successfully used in any TCM system.

3.3. Signal feature integration into tool wear evaluation

After the first tool life, a direct relationship $SF_{Tf}(\Delta T)$ (see Fig. 6) is determined for each selected signal feature. During the subsequent tool lives, when the system works in monitoring mode, it estimates the used-up portion of the tool life in two stages. In the first stage, the ΔTs are evaluated separately using each SF. The SF_{Tf} array is searched for the SF value closest to the measured value, starting with the value obtained in the previous, final ΔT estimation (in the second stage). In the second stage, the ΔT estimations obtained in the first stage are averaged.

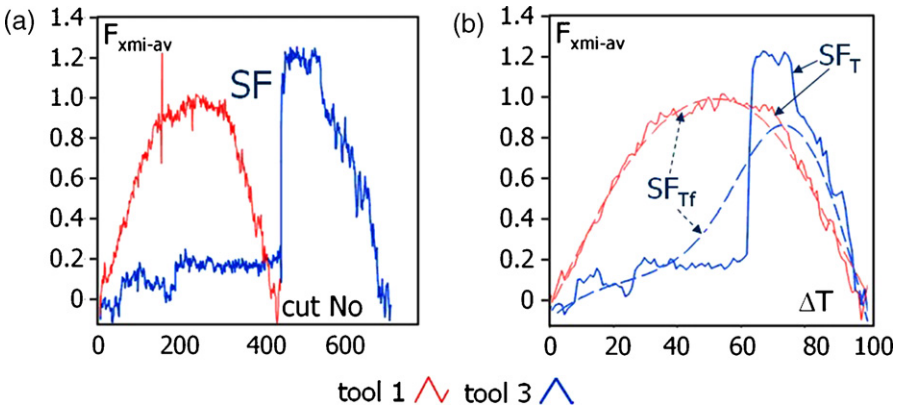

Fig. 6. SF processing in the described TCM system.

Table 1
Signal features selected by the TCM system after training on single tool data.

Tool	Selected signal features
1	$F_{zmx\text{-}av}$ F_{xsumP} F_{zmi} AE_{av} F_{zsumP} $AE_{bgmi\text{-}av}$ F_{xmddY} AE_{mdmi} F_{xmdmi} F_{xmdrms} $AE_{mdmi\text{-}av}$ AE_{mdrg} F_{xmdsd} F_{ymdmi} $F_{xmdmi\text{-}av}$ F_{yrms} AE_{bgdY} F_{ydY} F_{xbgrms} $F_{zbgPedg}$ F_{ybgmi} F_{ymddY} $F_{xbgmi\text{-}av}$ $F_{xmdrelP}$ $F_{xmdmx\text{-}av}$ F_{yPrpm} F_{ysd} $F_{ymi\text{-}av}$ F_{yrelP} F_{ybgdY} F_{ymdmx} $F_{ymdrelP}$ $F_{ymdmi\text{-}av}$ F_{zrelP} F_{ymdrg}
2	F_{zmi} F_{zdY} F_{xmi} F_{zmdmx} F_{zrelP} F_{xdY} $F_{xmi\text{-}av}$ F_{ymi} F_{xbgsd} F_{xmdsd} $F_{xmdPrpm}$ AE_{mdmi} $F_{ybgPedg}$ $F_{xbgPrpm}$ AE_{bgmi} F_{ymdmx} AE_{bgdY} AE_{mdrms} AE_{av} F_{ymx} $F_{ybgrelP}$ F_{xrms} F_{ymdsd} F_{ybgmx} F_{xmdrms} $AE_{mx\text{-}av}$ AE_{bgmx} F_{ybgrms} $AE_{bgmi\text{-}av}$ AE_{bgrg} AE_{mdmx} AE_{mddY} $F_{ybgmx\text{-}av}$ $AE_{mdmi\text{-}av}$ F_{ymdrms} $F_{ymx\text{-}av}$ AE_{mdrg} F_{yrms} F_{ymdrg}
3	$F_{zmdmx\text{-}av}$ $F_{xmdsumP}$ $F_{xmx\text{-}av}$ F_{zmdmi} $F_{xmdmx\text{-}av}$ F_{xrms} $F_{ymi\text{-}av}$ F_{ymdmi} F_{ymdrms} F_{ydY} $F_{ymdmi\text{-}av}$ AE_{mdav} F_{xrg} F_{xPrpm} F_{ybgdY} F_{ybgmi} AE_{mddY} $F_{ybgmi\text{-}av}$ $F_{ybgmx\text{-}av}$ $F_{xbgPrpm}$ F_{xmddY} F_{xmdmi} F_{xsd} F_{xbgrms} $F_{ybgsumP}$
4	F_{zmdsd} F_{zmdmx} F_{zmdmi} F_{xmdmx} AE_{mddY} $F_{zbgmi\text{-}av}$ AE_{mi} $AE_{mdmi\text{-}av}$ $F_{xbgPrpm}$ $F_{xmdrelP}$ F_{ymdmi} F_{yav} AE_{rms} $F_{ymdmi\text{-}av}$ $F_{ybgmi\text{-}av}$ $AE_{mi\text{-}av}$ F_{zrelP} AE_{mx} AE_{bgmx}

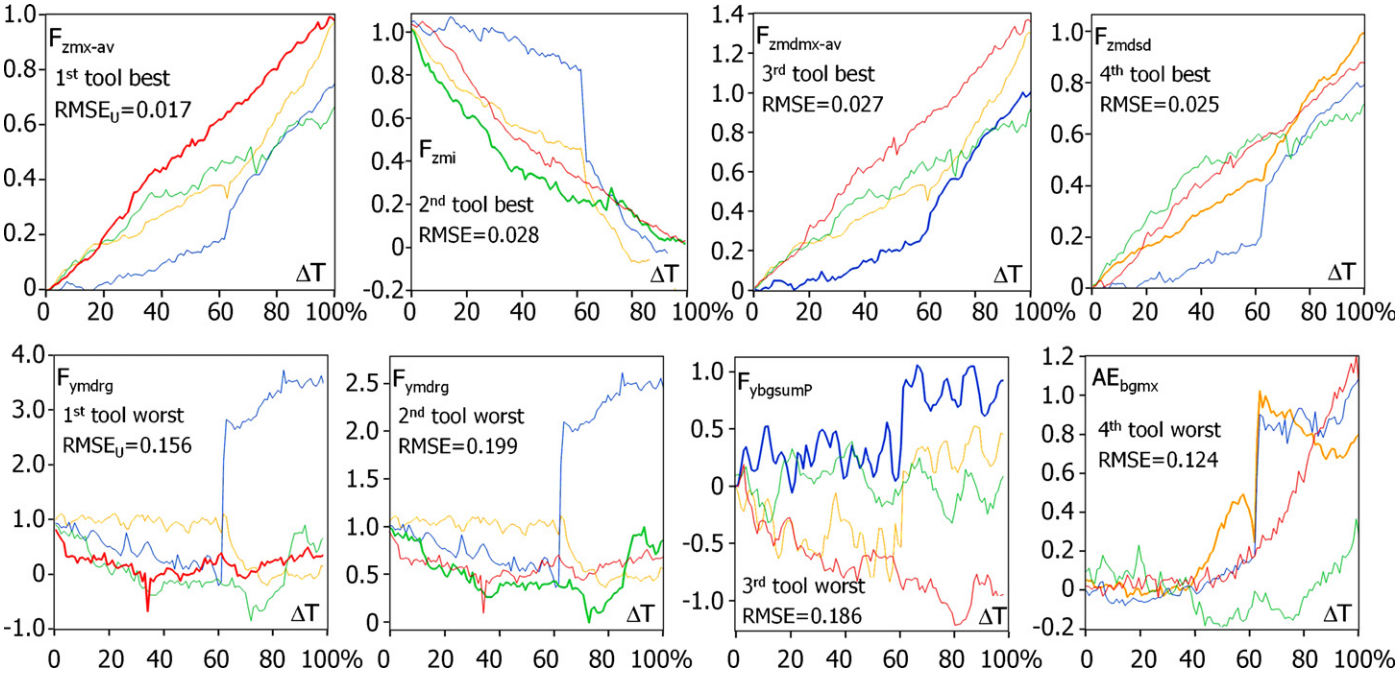

Fig. 7. Examples of SFs selected while training the system with subsequent tools.

The final results of the system testing for all four cases, i.e., using different tool lives as the first (training) tool, are presented in Fig. 8 as the used-up part a of tool's life evaluated by the system (ΔT_{ev}) vs. actual ΔT. Errorless estimation is shown by the straight, dashed line, and deviations from this line are presented as the RMSE. As can be seen, despite very disturbed input SF values as seen in Figs. 5 and 7, tool condition estimation appeared to be quite good, irrespective of which tool life was used for training the system. The best results were obtained when the system was trained on the fourth tool, but the others show very good results as well.

As a dynamometer is expensive and not always easy to install, it is worth trying to eliminate it and to monitor tool wear using the AE signal only. The TCM system was thus fed with the AE_{RMS} signal only, and the procedure was exactly the same as described above. The results are presented in Fig. 9, analogous to Fig. 8.

Because the AE signal behaved untypically during the second tool life, evaluation of this tool life was evidently poor, with the

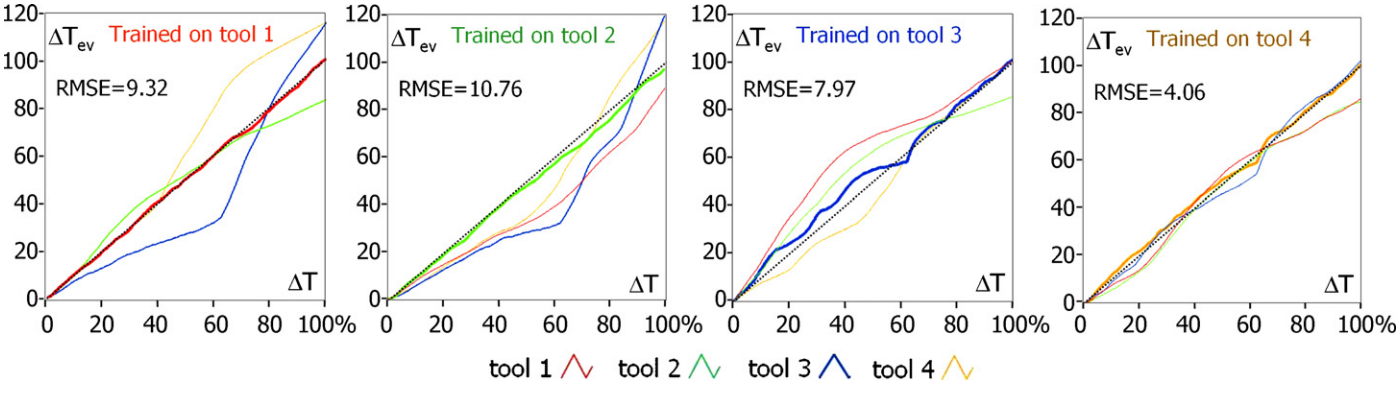

Fig. 8. Used-up portion of tool life evaluated by the TCM system (ΔT_{ev}) vs. actual portion (ΔT) after training on selected tool lives and testing on others.

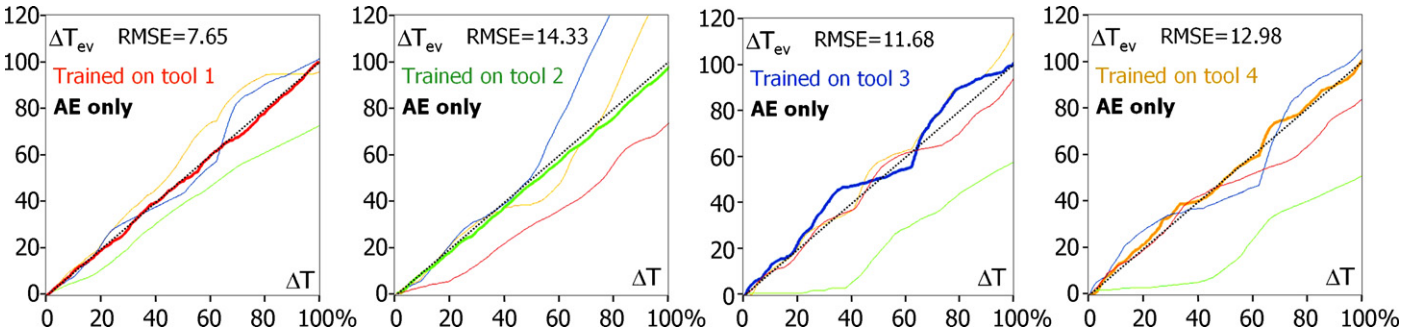

Fig. 9. Used-up portion of tool life evaluated by the TCM system (ΔT_{ev}) vs. actual portion (ΔT) after training on selected tool lives and testing on others, based on AE signal only.

exception when this tool life was used for training. In any case the obtained results can be considered as satisfactory.

4. Summary

Cutting forces and acoustic emission signals provide very useful information for tool condition monitoring in micro-milling. An acoustic emission signal is free from mechanical disturbances like resonance vibrations, which is very important in micro-machining applications, where spindle speeds have to be very high due to the small tool diameter. Despite the small material removal rate in micromachining, the obtained AE signal was strong, easy to register, and showed a very short reaction time to the tool–workpiece contact, which makes it a very good means of detecting this contact and monitoring the integrity of the cutting process.

The cutting force signals acquired in this study were severely disturbed by resonance vibrations in the dynamometer. In spite of this, the measurements still appeared to be very useful in tool wear monitoring.

Signal feature integration in tool condition monitoring minimizes the diagnosis uncertainty, reducing the randomness in one SF and providing a more reliable tool condition estimation. The number of SFs should be as big as possible, preferably originating from different sensors. Very good results can be achieved using cutting forces and acoustic emission. TCM based on AE only, as an AE sensor is much less expensive and easier to install, is worse than that based on four signals, yet still provides acceptable results.

Tool condition monitoring strategies should be tested on tool lives that are different from the tool life used to train the system. A good practice is to repeat the test for every available tool life to avoid selecting the best results, while ignoring the worst, less satisfactory results.

Acknowledgments

This research has been supported by the EU, FP6 Project "Launch-Micro", and the Polish Ministry of Science and Higher Education, project "Multi-parameter Tool Condition Monitoring". The authors sincerely thank M. Nejman and P.X. Aristimuno for their valuable contributions to the preparation of this paper.

References

[1] Dornfeld, D., Min, S., Takeuchi, Y., 2006, Recent Advances in Mechanical Micromachining, Annals of the CIRP, 55/2: 745–768.
[2] Tansel, I.N., Arkan, T.T., Bao, W.Y., et al, 2000, Tool Wear Estimation in Micro-Machining, International Journal of Machine Tools Manufacturing, 40:599–608.
[3] Lee, D.E., Hwang, I., Valente, C.M.O., Oliveira, J.F.G., Dornfeld, D.A., 2006, Precision Manufacturing Process Monitoring with Acoustic Emission, International Journal of Machine Tools Manufacturing, 46:176–188.
[4] Byrne, G., Dornfeld, D., Inasaki, I., König, W., Teti, R., 1995, Tool Condition Monitoring (TCM)—The Status of Research and Industrial Application, Annals of the CIRP, 44/2: 541–567.
[5] Jemielniak, K., 1999, Commercial Tool Condition Monitoring Systems, Journal of Advanced Manufacturing Technology, 15:711–721.
[6] Rehorn, A.G., Jiang, J., Orban, P.E., 2005, State-of-the-Art Methods and Results in Tool Condition Monitoring: A Review, Journal of Advanced Manufacturing Technology, 26:693–710.
[7] Sun, J., Hong, G.S., Wong, Y.S., Rahman, M., Wang, Z.G., 2006, Effective Training Data Selection in Tool Condition Monitoring System, International Journal of Machine Tools Manufacturing, 46:218–224.
[8] Kuo, R.J., Cohen, P.H., 1999, Multi-Sensor Integration for On-Line Tool Wear Estimation Through Radial Basis Function Networks and Fuzzy Neural Network, Neural Networks, 12/2:355–370.
[9] Jemielniak, K., 2006, Tool Wear Monitoring Based on a Non-Monotonic Signal Feature, Journal of Engineering Manufacture, 220/B2:163–170.
[10] Jemielniak, K., Bombiński, S., 2006, Hierarchical Strategies in Tool Wear Monitoring, Journal of Engineering Manufacture, 223/B3:375–382.
[11] Park, S.S., Altintas, Y., 2004, Dynamic Compensation of Spindle Integrated Force Sensors with Kalman Filter, ASME Journal of Dynamic Systems Measurement and Control, 126:443–452.
[12] Chae, J., Park, S.S., 2006, High Frequency Bandwidth Measurements of Micro-Cutting Forces, 2nd CIRP International Conference on High Performance Cutting, . Paper 56; Vancouver 2006.